Energy & Environmental Science

COMMUNICATION

Cite this: *Energy Environ. Sci.*, 2016, **9**, 135

Received 13th November 2015,
Accepted 9th December 2015

DOI: 10.1039/c5ee03460d

www.rsc.org/ees

High-performance ternary blend all-polymer solar cells with complementary absorption bands from visible to near-infrared wavelengths†

Hiroaki Benten,* Takaya Nishida, Daisuke Mori, Huajun Xu, Hideo Ohkita and Shinzaburo Ito*

We developed high-performance ternary blend all-polymer solar cells with complementary absorption bands from visible to near-infrared wavelengths. A power conversion efficiency of 6.7% was obtained with an external quantum efficiency over 60% both in the visible and near-infrared regions. Our results demonstrate that the ternary blend all-polymer systems open a new avenue for accelerating improvement in the efficiency of non-fullerene thin-film polymer solar cells.

Broader context

Continued expansion of energy consumption worldwide necessitates future global energy that is based on limitless resources and that generates less greenhouse gases than fossil-fuel-based energy sources. The use of photovoltaic energy is a promising approach that can solve the energy problems we will face in the foreseeable future. Recently, organic photovoltaics (OPVs) have gained increasing attention as an inexpensive source of renewable energy owing to their unique advantages including high throughout and large-area production with low-cost printing processes. Among the OPVs, all-polymer solar cells based on a blend of two types of conjugated polymers acting as an electron donor (hole transport) and an electron acceptor (electron transport) have numerous potential advantages over conventional fullerene-based solar cells, though the polymer/polymer blend systems still lag behind their polymer/fullerene counterparts in power conversion efficiencies (PCEs). Herein, we report high-performance ternary blend all-polymer solar cells in which a wide-bandgap visible polymer is introduced as a third polymer into a low-bandgap near-infrared donor/acceptor binary polymer blend. Owing to the complementary absorption bands of the ternary blend, the PCE is improved up to 6.7% with an external quantum efficiency over 60% both in the visible and near-infrared regions. Our results demonstrate that the ternary blend all-polymer solar cells open a new avenue for accelerating improvement in the efficiency of non-fullerene thin-film OPVs.

Organic photovoltaics have gained increasing attention as an inexpensive source of renewable energy owing to their unique advantages including high throughout and large-area production with low-cost printing processes.[1] The power conversion efficiencies (PCEs) of organic thin-film solar cells have made significant progress over the past decade, and approached 10% in single-junction cells.[2] The most widely studied solar cells consist of a bulk-heterojunction (BHJ) structure in which a conjugated polymer is mixed with a low-molecular-weight fullerene derivative.[3] In the systems, the conjugated polymer acts as an electron donor and the fullerene derivative acts as an electron acceptor. On the other hand, polymer/polymer blend BHJ solar cells that utilize conjugated polymers as both an electron donor and an electron acceptor have recently attracted much attention because they have numerous potential advantages over conventional polymer/fullerene BHJ solar cells. In particular, the flexible molecular design of not only the donor but also the acceptor material affords a large scope for tuning the optical, electronic, morphological, and mechanical properties of their blended films, which should give an optimal device performance superior to that of polymer/fullerene blend BHJ solar cells. While the PCE of polymer/polymer BHJ solar cells was limited to around 2% until 2012,[4] it has steeply increased owing to the development of low-bandgap polymer acceptors, which show both high electron mobility (μ_e) and high electron affinity similar to those of fullerenes.[5] Very recently, PCE values approaching 6–7%[6–8] and 7.7%[9] have been reported.

One of the promising strategies for achieving efficient performance of the polymer/polymer BHJ solar cells is to use donor and acceptor polymers that exhibit efficient light-absorption capabilities at near-infrared (NIR) wavelengths where the photon flux of the solar spectrum is at its highest levels. This is important for obtaining large short-circuit current density (J_{SC}) values even for the thin films optimal for charge carrier collection. Recently, we developed polymer/polymer BHJ solar cells based on a pair of low-bandgap donors and acceptors, poly[4,8-bis(5-(2-ethylhexyl)thiophen-2-yl)benzo[1,2-b;4,5-b′]dithiophene-2,6-diyl-*alt*-(4-(2-ethylhexyl)-3-fluorothieno[3,4-b]thiophene-)-2-carboxylate-2-6-diyl] (PBDTTT-EF-T) and poly{[*N*,*N*′-bis(2-octyldodecyl)-naphthalene-1,4,5,8-bis(dicaroximide)-2,6-diyl]-*alt*-5,5′-(2,2′-bithiophene)}

Department of Polymer Chemistry, Graduate School of Engineering, Kyoto University, Katsura, Nishikyo, Kyoto 615-8510, Japan.
E-mail: benten@photo.polym.kyoto-u.ac.jp, sito@photo.polym.kyoto-u.ac.jp

† Electronic supplementary information (ESI) available. See DOI: 10.1039/c5ee03460d

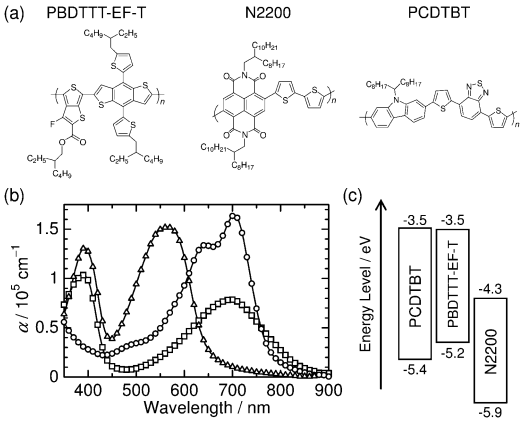

Fig. 1 (a) Chemical structures of PBDTTT-EF-T, N2200, and PCDTBT. (b) Absorption coefficients α of PBDTTT-EF-T (circles), N2200 (squares), and PCDTBT (triangles) measured in neat film spin-coated from chlorobenzene. (c) Energy level diagram for neat films of each polymer. The HOMO levels were determined by photoelectron yield spectroscopy, whereas the LUMO levels were estimated by adding the optical energy gap calculated from the 0–0 transition to the HOMO energy (ESI,† Fig. S1).

[P(NDI2OD-T2); Polyera ActivInk™ N2200], respectively (Fig. 1a).[7] The PBDTTT-EF-T/N2200 active layer having a thickness of as low as 100 nm can absorb over 90% of the incident sunlight at a wavelength of around 700 nm, resulting in an average J_{SC} of 13 mA cm^{-2} and a PCE of 5.5%.[7] Further, the generation and collection efficiencies of free charge carriers are each estimated to be 80% for the PBDTTT-EF-T/N2200 blend systems,[7] which is as high as those of efficient polymer/fullerene BHJ solar cells.[3] On the other hand, as shown in Fig. 1b, the combination of low-bandgap donor and acceptor polymers inevitably results in an weak light absorptivity in the visible region, owing to the intrinsic narrow absorption bandwidth of organic semiconductors. It should be noted that the polymer/polymer BHJ solar cells with the highest level of PCEs reported in the recent literature[8–10] also face a comparable challenge: the external quantum efficiency (EQE) in the visible region is relatively low although the EQE in the NIR region shows excellent values higher than 60%. As a consequence, the PCE still continues to be lower than state-of-the-art polymer/fullerene solar cells.[2] Therefore, further improvement in the PCE requires new design strategies that can complement the weak absorption in the visible range, while taking full advantage of the excellent photovoltaic conversion characteristics of these highly efficient low-bandgap donor/acceptor polymer blends.

The ternary blend polymer solar cell, which is fabricated by blending a second polymer donor or a dye molecule into a binary blend of a polymer donor and a [6,6]-phenyl-C_{61}-butyric acid methyl ester (PCBM) acceptor, is emerging as a fascinating alternative for broadening the absorption bandwidth of the photoactive layer.[11,12] Owing to the advantage of overcoming the absorption limitation, the ternary blends based on wide- and low-bandgap donor polymers and PCBM have been investigated to achieve a PCE higher than that of the original binary polymer/PCBM solar cells.[13,14] However, this concept has not been widely applied to enhance the efficiency of polymer/polymer BHJs,[15] because such ternary blend systems require not only complementary absorption bands but also sufficient free carrier generation and effective charge transport properties of both constituent binary blends. Unlike the case with polymer/PCBM systems, there are few such ideal binary polymer/polymer blends that work well individually at different wavelength ranges, while they share the common polymer acceptor.

In this study, we have designed ternary blend all-polymer solar cells in which a wide-bandgap polymer, poly[*N*-9′-heptadecanyl-2,7-carbazole-*alt*-5,5-(4′,7′-di-2-thienyl-2′,1′,3′-benzothiadiazole)] (PCDTBT), is introduced as a second donor into the highly efficient low-bandgap PBDTTT-EF-T/N2200 blend. We found that PCDTBT can contribute to efficient photocurrent generation in the ternary blends even though photovoltaic performance is poor for PCDTBT/N2200 binary blends. As a result, we have developed high-performance ternary blend all-polymer solar cells with much better efficiency than the PBDTTT-EF-T/N2200 binary blend, with an enhanced EQE of 65–70% even at visible wavelengths, and with a PCE of 6.65%. The values are the highest reported for ternary blend all-polymer BHJ solar cells. Furthermore, these results provide the first example of enhanced performance in ternary blend all-polymer systems based on highly efficient polymer/polymer BHJ solar cells.

As shown in Fig. 1b, the ternary blends are capable of providing broad and strong absorption covering the range of wavelengths from the visible to NIR regions because PCDTBT has an absorption band in the visible region that is complementary to the other two polymers, PBDTTT-EF-T and N2200. The PBDTTT-EF-T/N2200 binary BHJ solar cells were fabricated according to the method described in the previous report and used as a reference for the ternary blends.[7] The PBDTTT-EF-T/N2200 active layer was spin-coated from a chlorobenzene solution onto poly(3,4-ethylenedioxythiophene):poly(4-styrenesulfonate)-coated (PEDOT:PSS-coated) indium–tin-oxide (ITO) substrates. The weight ratio of PBDTTT-EF-T to N2200 was 1 : 1 and the film thickness of the PBDTTT-EF-T/N2200 blend was optimized at ~100 nm.[7] In the case of the PBDTTT-EF-T/N2200/PCDTBT ternary BHJ solar cells, PCDTBT was added to the PBDTTT-EF-T/N2200 binary blend, such that the weight fraction of PCDTBT in the ternary blends ranged from 0 to 30 wt%. Here, the PBDTTT-EF-T:N2200 weight ratio remained constant at 1 : 1, and the absorbances of PBDTTT-EF-T and N2200 were adjusted to the same value as that of the PBDTTT-EF-T/N2200 binary blend. Therefore, as shown in Fig. 2a, the thickness of the ternary blend active layer increases with an increase in the amount of PCDTBT. The absorption spectra of the PBDTTT-EF-T/N2200 binary and PBDTTT-EF-T/N2200/PCDTBT ternary blends are shown in Fig. 2b; the absorbance in the visible region at around 400 nm and 450–650 nm increased upon the addition of PCDTBT, whereas the absorbances of both PBDTTT-EF-T and N2200 at wavelength longer than 670 nm remained the same. As controls, the PCDTBT/N2200 binary and PBDTTT-EF-T/PCDTBT binary BHJ solar cells were also fabricated by spin-coating from chlorobenzene solutions onto the PEDOT:PSS films. The weight ratio of PCDTBT to N2200 and that of PBDTTT-EF-T to PCDTBT was 1 : 1 and the film thickness of these binary blends was adjusted to be ~100 nm.

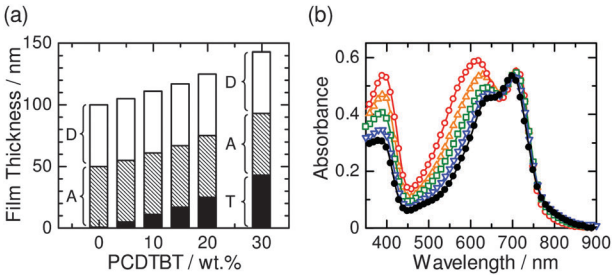

Fig. 2 (a) Estimated total film thickness and composition ratio of the constituent polymers in the PBDTTT-EF-T/N2200/PCDTBT ternary blend films plotted against the loading amount of PCDTBT. D, A, and T represent PBDTTT-EF-T, N2200, and PCDTBT, respectively. (b) Absorption spectra of PBDTTT-EF-T/N2200 binary blend (solid circles) and PBDTTT-EF-T/N2200/PCDTBT ternary blend films that contained 5 wt% (inverted triangles), 10 wt% (squares), 20 wt% (triangles), and 30 wt% (open circles) of PCDTBT.

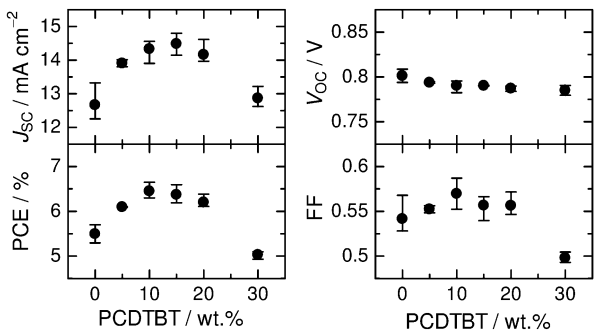

Fig. 3 Photovoltaic parameters (J_{SC}, V_{OC}, FF, and PCE) of PBDTTT-EF-T/N2200 binary and PBDTTT-EF-T/N2200/PCDTBT ternary BHJ solar cells with different amounts of PCDTBT loading. Each value is an average over a minimum of 10 devices.

Fig. 3 shows the dependence of the device performance of the PBDTTT-EF-T/N2200/PCDTBT ternary blend solar cells on the amount of PCDTBT loading. The PBDTTT-EF-T/N2200 binary blend used as a reference device gave an average PCE of 5.49% with a J_{SC} of 12.7 mA cm^{-2}, an open-circuit voltage (V_{OC}) of 0.801 V, and a fill factor (FF) of 0.542. It is clear from this figure that J_{SC} is enhanced significantly with an increase in the amount of PCDTBT and it reaches 14.48 mA cm^{-2} for the ternary blend containing 15 wt% PCDTBT. The value of V_{OC} was nearly constant at around 0.80 V and the FF values were as high as 0.54–0.57, regardless of the amount of PCDTBT in the range of 0–20 wt%. As a result, the PCE increased in the same fashion as J_{SC}, with maximum values achieved at 10–15 wt% PCDTBT. The improvement in PCE is thus primarily due to the increase in J_{SC} from the binary device. On the other hand, PCDTBT loadings of 30 wt% have a detrimental effect on the device performance, with decreases in both J_{SC} and FF and consequently, PCE.

Fig. 4 shows the current density–voltage (J–V) curves and the EQE spectrum of the PBDTTT-EF-T/N2200/PCDTBT ternary (open circles) BHJ solar cell with the best PCE of 6.65% under AM 1.5G illumination with an intensity of 100 mW cm^{-2}. The best photovoltaic performance was obtained for the ternary device with 10 wt% PCDTBT; the device parameters were a J_{SC} of 14.4 mA cm^{-2}, an V_{OC} of 0.790 V, and a FF of 0.583. For comparison, J–V curves and EQE spectra for the PBDTTT-EF-T/N2200 binary (solid circles) and PCDTBT/N2200 binary (open squares) blends are also shown in the figure, and the photovoltaic parameters of these devices are summarized in Table 1. Herein, we note that the device performance of the PBDTTT-EF-T/PCDTBT binary blend was much poorer than that of the PCDTBT/N2200 binary blend, with a J_{SC} of 0.118 mA cm^{-2} and a PCE of 0.042% (ESI,† Fig. S2), indicating that PBDTTT-EF-T/PCDTBT heterojunctions are unsuitable for charge generation. The origin of the enhanced J_{SC} for the ternary blends can be deduced from the EQE spectra. For the PBDTTT-EF-T/N2200 binary device, the EQEs were limited to 50% in the visible range from 500 to 600 nm. For the ternary device, the EQEs were improved noticeably mainly in the visible wavelengths, approaching values as high as 65–70%. Improvement in the EQEs at the PCDTBT absorption wavelength demonstrates that the increase in J_{SC} for the ternary device is caused by the additional light absorption of PCDTBT. In addition, we note that the existence of EQEs higher than 60% at the NIR wavelengths reveals that the photovoltaic conversion through direct light absorption by both PBDTTT-EF-T and N2200 host polymers remained as excellent as that of the individually optimized PBDTTT-EF-T/N2200 binary blend, which is an essential prerequisite for improving overall device efficiency.

As shown in Fig. 5, the photoluminescence (PL) spectrum of PCDTBT overlaps well with the absorption spectra of both PBDTTT-EF-T and N2200, giving a Förster radius (R_0) of 3.5 nm for PCDTBT to PBDTTT-EF-T and 3.3 nm for PCDTBT to N2200 (ESI,† Fig. S3).[16] Therefore, in addition to the enhanced light absorption by PCDTBT, in the ternary blends, resonant Förster energy transfer should occur from the wide-bandgap visible polymer PCDTBT to the low-bandgap NIR host polymers, PBDTTT-EF-T and N2200, after the light-absorption by PCDTBT.[14,17] The energy transfer enables long-range transport of PCDTBT excitons directly to both PBDTTT-EF-T and N2200. To unravel the mechanism whereby our ternary blend system functioned

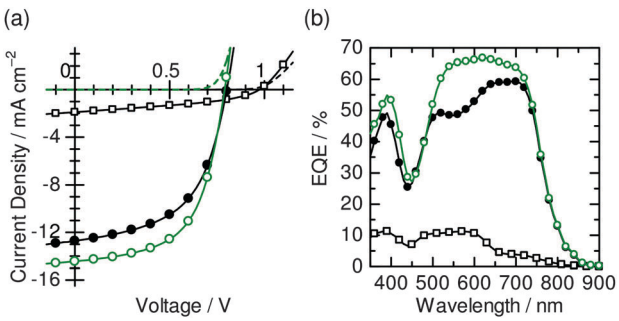

Fig. 4 (a) J–V characteristics of PBDTTT-EF-T/N2200/PCDTBT ternary (open circles), PBDTTT-EF-T/N2200 binary (solid circles), and PCDTBT/N2200 binary (open squares) BHJ solar cells measured under AM1.5G illumination from a calibrated solar simulator with an intensity of 100 mW cm^{-2}. The broken lines represent the J–V characteristics under dark conditions. The loading amount of PCDTBT in the ternary blend was 10 wt%. (b) EQE spectra of the devices: PBDTTT-EF-T/N2200/PCDTBT (open circles), PBDTTT-EF-T/N2200 (solid circles), and PCDTBT/N2200 (open squares).

Table 1 Photovoltaic parameters of the PBDTTT-EF-T/N2200/PCDTBT ternary, PBDTTT-EF-T/N2200 binary, and PCDTBT/N2200 binary BHJ solar cells. The PCDTBT loading amount in the ternary blend was 10 wt%. The J_{SC} calculated from the EQE spectrum, and the error between calculated (calc.) and measured J_{SC} is also shown

	Device[a]	J_{SC} (mA cm^{-2})	V_{OC} (V)	FF	PCE (%)	J_{SC} (calc.) (mA cm^{-2})	Error (%)
Ternary	PBDTTT-EF-T/N2200/PCDTBT	14.4 (14.3 ± 0.18)	0.790 (0.790 ± 0.00)	0.583 (0.570 ± 0.01)	6.65 (6.45 ± 0.11)	14.7	2.1
Binary	PBDTTT-EF-T/N2200	12.4 (12.7 ± 0.24)	0.806 (0.801 ± 0.00)	0.568 (0.542 ± 0.01)	5.70 (5.49 ± 0.10)	12.8	3.2
Binary	PCDTBT/N2200	2.00 (1.76 ± 0.11)	0.970 (0.959 ± 0.06)	0.397 (0.370 ± 0.01)	0.77 (0.634 ± 0.06)	1.94	3.0

[a] The values are the photovoltaic parameters of solar cells with the highest PCEs. Averaged values over at least 14 devices are shown in parentheses.

so beautifully, we focus on the charge generation from the excited states of PBDTTT-EF-T and N2200 even when light is absorbed by PCDTBT because PCDTBT excitons should be collected to PBDTTT-EF-T and N2200 by long-range exciton transport as mentioned above. Indeed, the PL of PCDTBT was completely quenched in the ternary blends regardless of the loading amount of PCDTBT ranging from 0 to 30 wt%, suggesting that all of the PCDTBT excitons are utilized for the charge generation (ESI,† Fig. S4). Firstly, the PBDTTT-EF-T excited state is not quenched at the interface with PCDTBT, owing to the negligible energy offset between the lowest unoccupied molecular orbital (LUMO) levels of PBDTTT-EF-T and PCDTBT (Fig. 1c and ESI,† Fig. S5a, b). The non-quenching of PBDTTT-EF-T excitons at the heterojunction with PCDTBT is consistent with the result of negligible J_{SC} values for the PBDTTT-EF-T/PCDTBT binary device (ESI,† Fig. S2). Therefore, PBDTTT-EF-T excitons, which are generated both directly by the NIR-light absorption and indirectly through the energy transfer from PCDTBT, can be converted to free charge carriers at the PBDTTT-EF-T/N2200 interface as efficiently as those in the case of the PBDTTT-EF-T/N2200 binary blends. The holes and electrons are transported through the PBDTTT-EF-T and N2200 networks, respectively, to the electrodes. Secondly, the N2200 excited state is quenched to form charges at the interfaces with PCDTBT, owing to an energy offset of 0.5 eV between the highest occupied molecular orbital (HOMO) levels of N2200 and PCDTBT (Fig. 1c). Here, the hole transfer from the N2200 excited state to PCDTBT will proceed in competition with charge generation at the other PBDTTT-EF-T/N2200 interface.

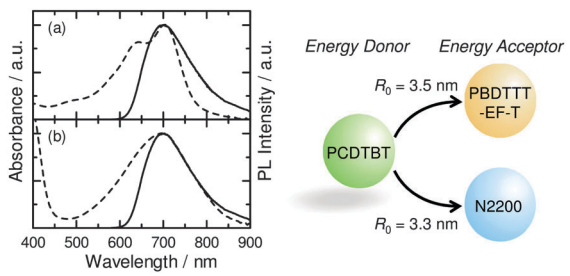

Fig. 5 (a) The absorption spectrum of PBDTTT-EF-T neat film (broken line) and the PL spectrum of PCDTBT neat film (solid line). (b) The absorption spectrum of N2200 neat film (broken line) and the PL spectrum of PCDTBT neat film (solid line). The strong overlap between the PCDTBT PL and the absorption bands of PBDTTT-EF-T and N2200 gave a Förster radius (R_0) of 3.5 nm and 3.3 nm, respectively (ESI,† Fig. S3)

The energy diagram suggests that the resulting holes on PCDTBT at the PCDTBT/N2200 interfaces can migrate towards PBDTTT-EF-T, owing to the preferred cascade alignment of the HOMO energy levels of PCDTBT and PBDTTT-EF-T (Fig. 1c). Therefore, they can be transported as holes of PBDTTT-EF-T through the high-hole-mobility PBDTTT-EF-T networks[7] to the electrode rather than being energetically trapped in relatively low-hole-mobility PCDTBT domains.[18] Consequently, the quenching of N2200 excitons at the PCDTBT/N2200 interface does not necessarily result in hole trapping but contributes to photocurrent generation. The efficient collection of PCDTBT excitons by long-range resonant energy transfer and the rational alignment of the HOMO–LUMO energy levels of PCDTBT that minimizes quenching losses of both PBDTTT-EF-T and N2200 excitons are keys for improving the EQEs in the visible region while retaining the excellent EQE values at the NIR wavelengths.

To confirm this scenario, we further examine the dependence of the photocurrent on the applied reverse (negative) voltage in the ternary blends with the best PCE. Fig. 6 shows the net photocurrent density (J_{ph}) of the PBDTTT-EF-T/N2200/PCDTBT ternary (open circles), PBDTTT-EF-T/N2200 binary (solid circles), and PCDTBT/N2200 binary (open squares) BHJ solar cells under AM 1.5G illumination at 100 mW cm^{-2}. Here, J_{ph} is given by $J_{ph} = J_L - J_D$, where J_L and J_D are the current densities under illumination and in the dark, respectively. It is worth noting that the PCDTBT/N2200 binary blend showed noticeable dependence of J_{ph} on the applied reverse voltage, suggesting poor efficiency of either charge dissociation (dissociation of bound electron–hole pairs) into free carriers or charge carrier transport, or both.[19] On the other hand, the PBDTTT-EF-T/N2200/PCDTBT ternary blend showed a weak dependence of J_{ph} on the applied reverse voltage, and the J_{ph} was saturated at reverse voltage higher than −8 V just as in the case of the PBDTTT-EF-T/N2200 binary blend,[7] suggesting that all of the photogenerated free charge carriers in the devices were collected at the reverse voltage higher than −8 V.[20] The increase in the reverse saturation photocurrent density $J_{ph,sat}$ (ΔJ_{SAT}) was 1.81 mA cm^{-2}, which agrees well with the increase in J_{SC} (ΔJ_{SC}) of 1.72 mA cm^{-2}. This agreement indicates that the additional free charge carriers resulting from the PCDTBT light absorption are free from bimolecular recombination loss and hence are efficiently collected under short circuit conditions. The overall charge collection efficiencies under short-circuit conditions, which are defined as the ratio of J_{SC} to $J_{ph,sat}$, were estimated to be as high as 84% in the ternary blend and 83% in the binary blend.

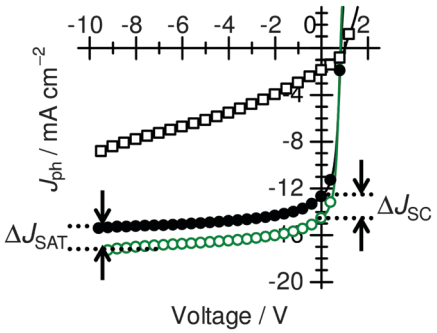

Fig. 6 Photocurrent density J_{ph} of the binary (solid circles) and ternary (open circles) blend solar cells as a function of the applied reverse voltage measured under AM1.5G illumination (100 mW cm^{-2}). The loading amount of the PCDTBT was 10 wt%. The J_{ph} values were obtained by subtracting the current density in the dark J_D from that under illumination J_L as $J_{ph} = J_L - J_D$.

These results demonstrate that the charge collection in the PBDTTT-EF-T/N2200/PCDTBT ternary BHJ solar cells can be as efficient as in the PBDTTT-EF-T/N2200 binary BHJ solar cells even though poor charge dissociation and/or transport is expected from the PCDTBT/N2200 binary BHJ solar cells. In other words, the PBDTTT-EF-T/N2200/PCDTBT ternary BHJ solar cell functioned well by taking full advantage of the excellent free carrier generation and transport capabilities of the PBDTTT-EF-T/N2200 binary BHJ.

Finally, we examine the dependence of $J_{SC}/J_{ph,sat}$ and charge carrier mobilities on the amount of PCDTBT loading. As shown in Fig. 7a, we found that the overall charge collection efficiency under short circuit conditions remained close to 80% even for the ternary blend containing 20 wt% PCDTBT. Fig. 7b shows μ_h and μ_e determined using the space-charge-limited current (SCLC) method with the Mott-Gurney equation.[21] The μ_h increased from 4.3×10^{-4} cm^2 V^{-1} s^{-1} in the PBDTTT-EF-T/N2200 binary blend to 1.3×10^{-3} cm^2 V^{-1} s^{-1} in the ternary blend containing 30 wt% PCDTBT, which is much larger than that of PCDTBT neat film (on the order of 10^{-5} cm^2 V^{-1} s^{-1}).[18] These results support our proposed mechanism that the bottleneck of charge-transport of the PCDTBT/N2200 binary device is overcome by energetically-feasible hole transfer from PCDTBT to PBDTTT-EF-T. On the other hand, the μ_e was found to decrease by an order of magnitude from 7.0×10^{-4} cm^2 V^{-1} s^{-1} in the binary blend to 6.9×10^{-5} cm^2 V^{-1} s^{-1} in the ternary blend containing 30 wt% PCDTBT, resulting in an imbalance between hole and electron mobilities. As shown in Fig. 3, the decrease in J_{SC} and FF was observed for the ternary blend containing 30 wt% PCDTBT. Such a detrimental effect may be attributed to reduced charge collection efficiency caused by the increased film thickness of ~150 nm and the decreased electron mobility.

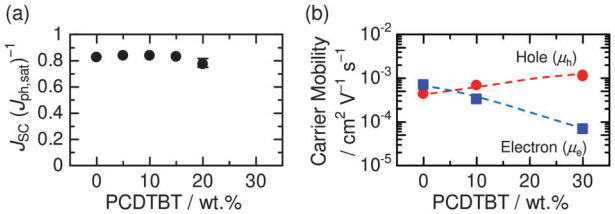

Fig. 7 (a) Overall charge collection efficiency under short-circuit conditions for the PBDTTT-EF-T/N2200 binary and PBDTTT-EF-T/N2200/PCDTBT ternary blend solar cells plotted against the PCDTBT loading amount. (b) The SCLC hole mobility (μ_h, circles) and electron mobility (μ_e, squares) of the PBDTTT-EF-T/N2200 binary and PBDTTT-EF-T/N2200/PCDTBT ternary blend films plotted against the amount of PCDTBT loading. The broken lines are observed by the naked eye.

As shown in Fig. 4 and 6, the second polymer donor PCDTBT forms BHJs with N2200 that exhibit limited photovoltaic performance and different V_{OC} values from the PBDTTT-EF-T/N2200 binary blend. However, our ternary blends composed of 0–20 wt% PCDTBT improved the PCE while retaining similar values of $J_{SC}/J_{ph,sat}$, V_{OC}, and FF to those of the PBDTTT-EF-T/N2200 host binary blend. The compositional dependence strongly suggests that PCDTBT contributed to the photocurrent generation as a visible sensitizer through efficient energy transfer for both PBDTTT-EF-T and N2200 rather than as a PCDTBT/N2200 device working in parallel with the PBDTTT-EF-T/N2200.[11] In this case, PCDTBT absorbs visible light but relies on both PBDTTT-EF-T and N2200 host polymers to generate and transport free charge carriers. As a result, improvement in the PCE can be achieved by taking full advantage of the excellent photovoltaic conversion characteristics of the PBDTTT-EF-T/N2200 binary blend.

Conclusions

We have demonstrated that the PCE of low-bandgap PBDTTT-EF-T/N2200 binary BHJ solar cells can be improved by introducing wide-bandgap PCDTBT to complement the weak absorption at visible wavelengths. For the ternary blend all-polymer BHJ solar cell containing 10 wt% PCDTBT, the EQEs at visible wavelengths were successfully increased up to 65–70%, and a PCE as high as 6.65% was obtained. These values are the highest reported for ternary blend all-polymer BHJ solar cells. In the ternary blends, PCDTBT excitons can be transported directly to both PBDTTT-EF-T and N2200 through long-range resonant Förster energy transfer, contributing to the photocurrent generation as a visible sensitizer. Consequently, light absorption by PCDTBT can lead to an increase in J_{SC}, by taking advantage of the excellent free carrier generation and transport characteristics of the PBDTTT-EF-T/N2200 binary blends. Our results demonstrate that the use of ternary blends composed of a wide-bandgap polymer along with an efficient low-bandgap donor/acceptor polymer blend is an effective strategy for achieving more efficient all-polymer BHJ solar cells. This approach should be applicable to the recently reported low-bandgap donor/acceptor polymer BHJ solar cells with the highest level of PCEs. The ternary blend all-polymer BHJs open a new avenue for accelerating improvement in the efficiency of non-fullerene thin-film polymer solar cells.

Acknowledgements

This work was supported by the JSPS KAKENHI Grant Number 26288060 and the CREST program of the Japan Science and Technology Agency.

Notes and references

1 R. Søndergaard, M. Hösel, D. Angmo, T. T. Larsen-Olsen and F. C. Krebs, *Mater. Today*, 2012, **15**, 36; S. B. Darling and F. You, *RSC Adv.*, 2013, **3**, 17633.

2 Z. He, C. Zhong, S. Su, M. Xu, H. Wu and Y. Cao, *Nat. Photonics*, 2012, **6**, 591; Z. He, B. Xiao, F. Liu, H. Wu, Y. Yang, S. Xiao, C. Wang, T. P. Russell and Y. Cao, *Nat. Photonics*, 2015, **9**, 174; Y. Liu, J. Zhao, Z. Li, C. Mu, W. Ma, H. Hu, K. Jiang, H. Lin, H. Ade and H. Yan, *Nat. Commun.*, 2014, **5**, 5293; M. A. Green, K. Emery, Y. Hishikawa, W. Warta and E. D. Dunlop, *Prog. Photovolt.: Res. Appl.*, 2015, DOI: 10.1002/pip.2728.

3 L. Bian, E. Zhu, J. Tang, W. Tang and F. Zhang, *Prog. Polym. Sci.*, 2012, **37**, 1292; C. J. Brabec, S. Gowrisanker, J. J. M. Halls, D. Laird, S. Jia and S. P. Williams, *Adv. Mater.*, 2010, **22**, 3839; G. Dennler, M. C. Scharber and C. J. Brabec, *Adv. Mater.*, 2009, **21**, 1323.

4 A. Facchetti, *Mater. Today*, 2013, **16**, 123.

5 X. Zhan, Z. Tan, B. Domercq, Z. An, X. Zhang, S. Barlow, Y. Li, D. Zhu, B. Kippelen and S. R. Marder, *J. Am. Chem. Soc.*, 2007, **129**, 7246; H. Yan, Z. Chen, Y. Zheng, C. Newman, J. R. Quinn, F. Dötz, M. Kastler and A. Facchetti, *Nature*, 2009, **457**, 679; E. Zhou, J. Cong, Q. Wei, K. Tajima, C. Yang and K. Hashimoto, *Angew. Chem., Int. Ed.*, 2011, **50**, 2799; X. Zhao and X. Zhan, *Chem. Soc. Rev.*, 2011, **40**, 3728.

6 L. Ye, X. Jiao, M. Zhou, S. Zhang, H. Yao, W. Zhao, A. Xia, H. Ade and J. Hou, *Adv. Mater.*, 2015, **27**, 6046.

7 D. Mori, H. Benten, I. Okada, H. Ohkita and S. Ito, *Energy Environ. Sci.*, 2014, **7**, 2939.

8 J. W. Jung, J. W. Jo, C. C. Chueh, F. Liu, W. H. Jo, T. P. Russell and A. K.-Y. Jen, *Adv. Mater.*, 2015, **27**, 3310; Y. J. Hwang, T. Earmme, B. A. E. Courtright, F. N. Eberle and S. A. Jenekhe, *J. Am. Chem. Soc.*, 2015, **137**, 4424; C. Lee, H. Kang, W. Lee, T. Kim, K. H. Kim, H. Y. Woo, C. Wang and B. J. Kim, *Adv. Mater.*, 2015, **27**, 2466; T. Kim, J. H. Kim, T. E. Kang, C. Lee, H. Kang, M. Shin, C. Wang, B. Ma, U. Jeong, T. S. Kim and B. J. Kim, *Nat. Commun.*, 2015, **6**, 8547.

9 Y. J. Hwang, B. A. E. Courtright, A. S. Ferreira, S. H. Tolbert and S. A. Jenekhe, *Adv. Mater.*, 2015, **27**, 4578.

10 C. Mu, P. Liu, W. Ma, K. Jiang, J. Zhao, K. Zhang, Z. Chen, Z. Wei, Y. Yi, J. Wang, S. Yang, F. Huang, A. Facchetti, H. Ade and H. Yan, *Adv. Mater.*, 2014, **26**, 7224.

11 L. Lu, M. A. Kelly, W. You and L. Yu, *Nat. Photonics*, 2015, **9**, 491; B. M. Savoie, S. Dunaisky, T. J. Marks and M. A. Ratner, *Adv. Energy Mater.*, 2014, 1400891; T. Ameri, P. Khoram, J. Min and C. J. Brabec, *Adv. Mater.*, 2013, **25**, 4245; L. Yang, L. Yan and W. You, *J. Phys. Chem. Lett.*, 2013, **4**, 1802; Y. C. Chen, C. Y. Hsu, R. Y. Y. Lin, K. C. Ho and J. T. Lin, *ChemSusChem*, 2013, **6**, 20; P. P. Khlyabich, B. Burkhart, A. E. Rudenko and B. C. Thompson, *Polymer*, 2013, **54**, 5267.

12 S. Honda, H. Ohkita, H. Benten and S. Ito, *Chem. Commun.*, 2010, **46**, 6596; S. Honda, T. Nogami, H. Ohkita, H. Benten and S. Ito, *ACS Appl. Mater. Interfaces*, 2009, **1**, 804; Y. Wang, B. Zheng, Y. Tamai, H. Ohkita, H. Benten and S. Ito, *J. Electrochem. Soc.*, 2014, **161**, D3093; H. Xu, T. Wada, H. Ohkita, H. Benten and S. Ito, *Sci. Rep.*, 2015, **5**, 9321; H. Xu, H. Ohkita, Y. Tamai, H. Benten and S. Ito, *Adv. Mater.*, 2015, **27**, 5868.

13 Y. Yang, W. Chen, L. Dou, W. H. Chang, H. S. Duan, B. Bob, G. Li and Y. Yang, *Nat. Photonics*, 2015, **9**, 190; K. Yao, Y. X. Xu, F. Li, X. Wang and L. Zhou, *Adv. Opt. Mater.*, 2015, **3**, 321; T. Ameri, J. Min, N. Li, F. Machui, D. Baran, M. Forster, K. J. Schottler, D. Dolfen, U. Scherf and C. J. Brabec, *Adv. Energy Mater.*, 2012, **2**, 1198; L. Yang, H. Zhou, S. C. Price and W. You, *J. Am. Chem. Soc.*, 2012, **134**, 5432; P. P. Khlyabich, B. Burkhart and B. C. Thompson, *J. Am. Chem. Soc.*, 2012, **134**, 9074.

14 Y. Wang, H. Ohkita, H. Benten and S. Ito, *Phys. Chem. Chem. Phys.*, 2015, **17**, 27217; V. Gupta, V. Bharti, M. Kumar, S. Chand and A. J. Heeger, *Adv. Mater.*, 2015, **27**, 4398.

15 Y. J. Hwang, B. A. E. Courtright and S. A. Jenekhe, *MRS Commun.*, 2015, **5**, 229.

16 T. Förster, *Discuss. Faraday Soc.*, 1959, **27**, 7; I. B. Berlman, *Energy Transfer Parameters of Aromatic Compounds*, Academic Press, New York and London, 1973, pp. 27–32.

17 Y. Liu, M. A. Summers, C. Edder, J. M. J Fréchet and M. D. McGehee, *Adv. Mater.*, 2005, **17**, 2960; S. R. Scully, P. B. Armstrong, C. Edder, J. M. J. Fréchet and M. D. McGehee, *Adv. Mater.*, 2007, **19**, 2961.

18 K. K. H. Chan, S. W. Tsang, H. K. H. Lee, F. So and S. K. So, *Org. Electron.*, 2012, **13**, 850.

19 M. M. Mandoc, W. Veurman, L. J. A. Koster, B. Boer and P. W. M. Blom, *Adv. Funct. Mater.*, 2007, **17**, 2167.

20 V. D. Mihailetchi, L. J. A. Koster, P. W. M. Blom, C. Melzer, B. Boer, J. K. J. Duren and R. A. J. Janssen, *Adv. Funct. Mater.*, 2005, **15**, 795; V. D. Mihailetchi, H. Xie, B. Boer, L. J. A. Koster and P. W. M. Blom, *Adv. Funct. Mater.*, 2006, **16**, 699; P. W. M. Blom, V. D. Mihailetchi, L. J. A. Koster and D. E. Markov, *Adv. Mater.*, 2007, **19**, 1551.

21 G. G. Malliaras, J. R. Salem, P. J. Brock and C. Scott, *Phys. Rev. B: Condens. Matter Mater. Phys.*, 1998, **58**, R13411; Y. Shen, A. R. Hosseini, M. H. Wong and G. G. Malliaras, *ChemPhysChem*, 2004, **5**, 16.

